# Translational energy dependence of cross sections for reactions of $OH^-(H_2O)_n$ with $CO_2$ and $SO_2$

Peter M. Hierl[a] and John F. Paulson
*Air Force Geophysics Laboratory (AFSC), Hanscom Air Force Base, Massachusetts 01731*

(Received 2 November 1983; accepted 3 February 1984)

A tandem mass spectrometer has been used to measure cross sections for reactions of the solvated negative ions $OH^-(H_2O)_n$, where $0 \leqslant n \leqslant 3$, with the neutral molecules $CO_2$ and $SO_2$ over the range of reactant translational energy 0.15–25.0 eV (LAB). The reactions observed include solvent switching, collisional dissociation, and charge transfer. The exoergic solvent switching reactions are very rapid, having cross sections which exceed a hundred square Angstroms at low energies. These cross sections decrease approximately as $(\text{energy})^{-0.5}$ up to 1 eV and then decrease much more rapidly at higher collision energies. Estimates of bond dissociation energies for the cluster ions are derived from the measured translational energy thresholds for the endothermic collisional dissociation reactions.

## I. INTRODUCTION

The effect of reactant solvation upon the rates of gas phase ion–molecule reactions is a problem of both fundamental interest and practical importance. Knowledge of the effect of hydration upon the reactivity of ions, for example, is necessary for a complete understanding of the ion chemistry of the earth's atmosphere.[1,2] The problem is also of interest in radiation chemistry, in the study of ionic reactions in both polar and nonpolar solvents, and as a source of basic data on the energetics and mechanisms of gas phase reactions.

We report here cross sections for the reactions of the solvated anion $OH^-(H_2O)_n$, where $0 \leqslant n \leqslant 3$, with the neutral molecules $CO_2$ and $SO_2$ over the range of reactant translational energy 0.15–25.0 eV (LAB). These reactions are particularly important to the ion chemistry of the earth's atmosphere below 80 km, where considerable hydration of negative ions have been observed.[2,3] In addition, the reaction products $HCO_3^-$ and $HSO_3^-$ are often found in natural and industrial waters,[4] and their properties are also of interest with regard to various biological processes.[5]

In a previous study, Fehsenfeld and Ferguson[3] measured thermal energy rates coefficients in a flowing afterglow for the reactions of $OH^-(H_2O)_n$, where $2 \leqslant n \leqslant 4$, with $CO_2$ and $SO_2$. This study, however, provided no information on the energy dependence of the reaction rate and only limited information on the identity of the reaction products. A report on the reactions of $OH^-(H_2O)_n$ with $NO_2$ in the beam apparatus used in the present work has been published.[6]

## II. EXPERIMENTAL

The experiments reported here were carried out using the AFGL tandem mass spectrometer.[6,7] Reactant negative ions are formed indirectly by ion-neutral reactions in an electron-bombardment ion source. These ions are mass analyzed by a 2.54 cm radius, 90° magnetic sector mass spectrometer and are then accelerated or decelerated to the desired kinetic energy before entering the neutral gas collision chamber. Reactant and product ions emerging from this chamber are accelerated by a series of grids and mass analyzed in a 46 cm quadrupole mass filter before being counted with a particle multiplier and conventional nuclear pulse counting equipment.

Target gas pressure in the collision chamber is measured with a capacitance manometer. Since this pressure is typically maintained at $3 \times 10^{-3}$ Torr, and since the collision path length is 0.2 cm, single collision conditions obtain for all reactions studied.

Because the angular and velocity distributions of the product ions are generally unknown, but may differ considerably from one reaction to another (or even for the same reaction at different collision energies), the relative collection efficiencies of reactant and product ions are, in general, also unknown. No corrections for varying collection efficiencies have been applied to the data in calculating the cross sections reported here. We estimate[6] that appropriate multiplicative correction factors vary between unity and 2.5, being close to unity for all but electron transfer reactions and for atom transfer reactions at low ion energies.

The quadrupole mass filter used here is normally operated in the high transmission mode in order to reduce mass discrimination effects. A transmission correction factor is obtained experimentally by operating the mass filter first without mass resolution (i.e., as a high pass filter), and then with normal resolution for both reactant and product ion mass numbers.

In the studies of collisional dissociation, a problem arises because dissociation of the reactant ion can occur even at nominal translational energies below the thermodynamic threshold, due to collisions of the reactant ions with molecules of background gas as the former are accelerated into the quadrupole mass filter. To minimize this effect in these studies, the acceleration the ions undergo between the collision chamber and the first grid in the ion optics before the entrance to the quadrupole mass filter was reduced to 1 eV from its normal value of 150 eV.

Since this reduced but did not entirely eliminate the problem, the contribution from collisions with the background gas was determined by measuring the extent of frag-

[a] SCEEE Fellow/AFOSR Summer Faculty Research Associate (1980). Permanent Address: Department of Chemistry, University of Kansas, Lawrence, KS 66045.

 0021-9606/84/104890-11$02.10 

mentation that occurred even when no target gas was present in the collision chamber; this contribution was then subtracted from the dissociation rate observed when the target was present.

Typically, data for a particular reaction are obtained for a number $N$ of replicate runs in which the reactant and product ion intensities are measured at each of 30 to 50 selected collision energies covering the range 0.15 to 25 eV (LAB). For a given run cross sections are then calculated from the expression

$$\sigma = \frac{K_2 I_2 / K_1 I_1^{\circ}}{nL},$$

where $I_2$ is the total reactively scattered product ion intensity, $I_1^{\circ}$ is the incident reactant ion intensity (obtained by summing the intensities of all transmitted ions), $K_2/K_1$ is the ratio of transmission correction factors (this ratio ranged from 0.65 to 1.2 for the reactions reported here), $n$ is the number density of the reactant neutral gas, and $L$ is length of the reaction chamber.

For the reactions of $OH^- \cdot H_2O$ with $CO_2$ and $SO_2$, the cross sections obtained in the replicate runs ($N = 13$ and 9, respectively) were averaged and then plotted against the relative collision energy.[9] These runs were performed in 3–4 sets of 2–3 runs at widely spaced intervals over a period of two years. Results within a given set generally showed very good reproducibility; however, results from sets taken months apart sometimes differed by as much as a factor of 2.

Data for the reactions of $OH^-(H_2O)_2$, $OH^-(H_2O)_3$, and $HCO_3^-$ were obtained in a single set of measurements (with $N = 2$–5) performed over a period of about one month. These cross sections were normalized by the factor necessary to bring the $OH^- \cdot H_2O$ cross sections measured during this period into agreement with the $OH^- \cdot H_2O$ cross sections from all sets.

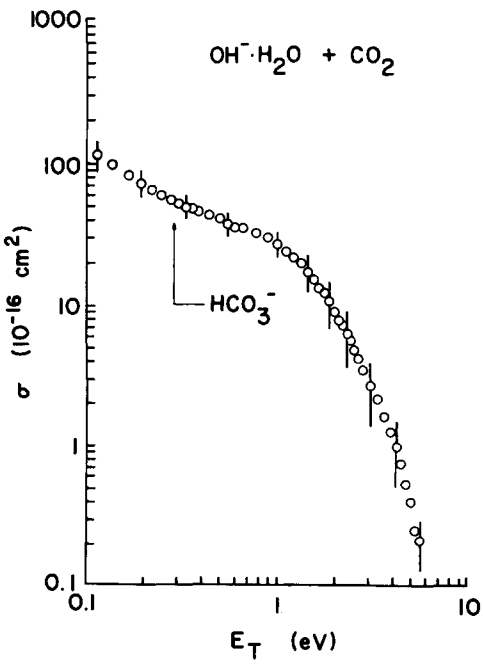


FIG. 1. Cross sections $\sigma$ for reaction (1) as a function of the relative collision energy $E_T$. Error bars on selected points represent standard deviations from the mean.

The calculation of thermal rate coefficients $k(T)$ from reaction cross sections is a difficult problem requiring a knowledge (usually unavailable) of the distribution of, and the cross section dependence on, both the internal and the translational energies of the reactants.[10] However, a phenomenological rate coefficient $k(v_r)$ appropriate to collisions at a relative velocity $v_r$, can be obtained from the relation $k(v_r) = v_r \sigma(v_r)$. The reaction cross sections measured in this study were converted to rate coefficients by application of this formula and extrapolated to thermal energies to obtain pseudo thermal rate coefficients. Although not identical to thermal rate coefficients, such monoenergetic rate coefficients serve two useful functions. First, extrapolation to thermal energy permits the results obtained in the present beam experiment to be compared with true thermal rate coefficients measured by other techniques, such as the flowing afterglow study by Fehsenfeld and Ferguson.[3] Second, comparison of the monoenergetic rate coefficient $k(v_r)$ with the calculated collision rate coefficient yields the reaction efficiency (i.e., the fraction of collisions which result in a particular reaction) as a function of collision energy.

## III. RESULTS

With $CO_2$ as the neutral reactant, data were obtained for the following reactions:

$$OH^-(H_2O) + CO_2 \rightarrow HCO_3^- + H_2O, \quad (1)$$

$$OH^-(H_2O)_2 + CO_2 \rightarrow HCO_3^- + 2H_2O \quad (2a)$$

$$\rightarrow HCO_3^-(H_2O) + H_2O, \quad (2b)$$

$$OH^-(H_2O)_3 + CO_2 \rightarrow HCO_3^- + 3H_2O \quad (3a)$$

$$\rightarrow HCO_3^-(H_2O) + 2H_2O \quad (3b)$$

$$\rightarrow HCO_3^-(H_2O)_2 + H_2O. \quad (3c)$$

The cross sections for these reactions are plotted vs the relative collision energy $E_T$ in Figs. 1–3. These cross sections are

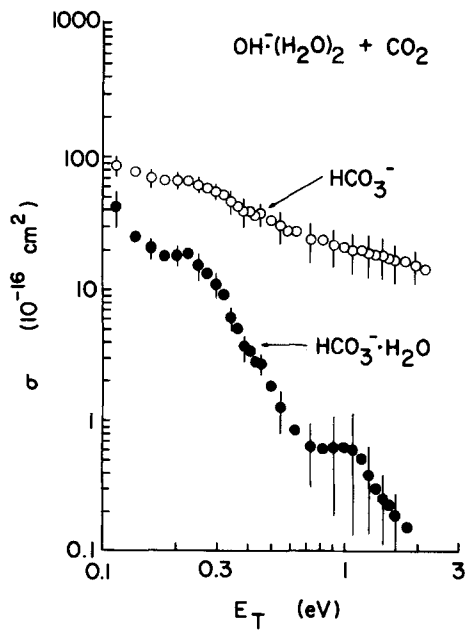


FIG. 2. Cross sections $\sigma$ for reactions (2a) ○ and (2b) ● as functions of the relative collision energy $E_T$.

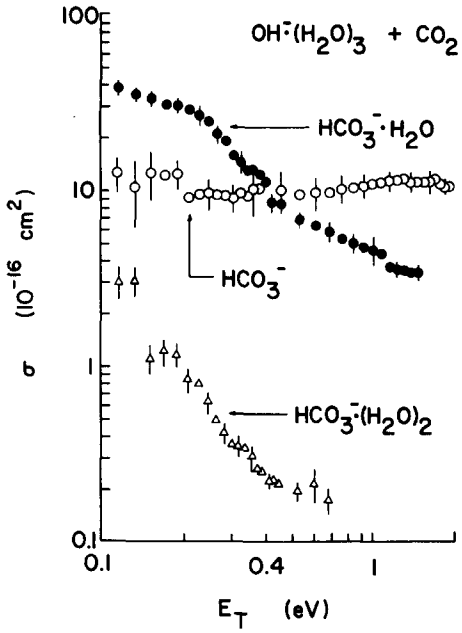


FIG. 3. Cross sections $\sigma$ for reactions (3a) ○, (3b) ●, and (3c) △ as functions of the relative collision energy $E_T$.

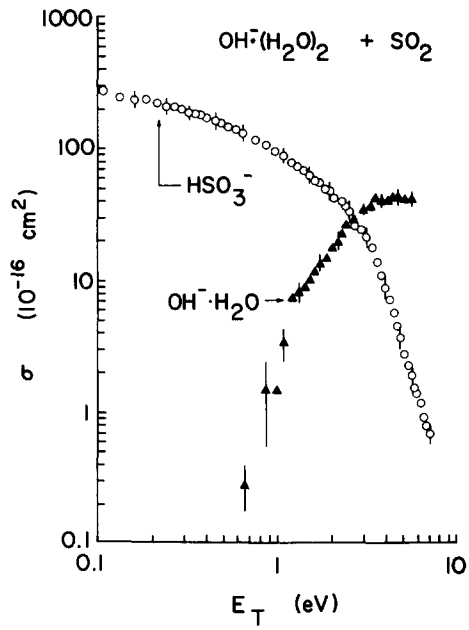


FIG. 5. Cross sections $\sigma$ for reactions (5a) ▲ and (5b) ○ as functions of the relative collision energy $E_T$.

subject to the uncertainties discussed previously; the uncertainties, which arise largely from differences in collection efficiencies of reactant and product ions, amount to about a factor of 2. The error bars shown in these and subsequent figures represent plus and minus one standard deviation from the mean value of the cross section derived from the $N$ replicate runs and thus provide a measure of the precision of these measurements.

With $SO_2$ as the neutral reactant, data were obtained for the following reactions:

$$OH^-(H_2O) + SO_2 \rightarrow OH^- + H_2O + SO_2 \quad (4a)$$
$$\rightarrow HSO_3^- + H_2O \quad (4b)$$

$$OH^-(H_2O)_2 + SO_2 \rightarrow OH^-(H_2O) + H_2O + SO_2 \quad (5a)$$
$$\rightarrow HSO_3^- + 2H_2O, \quad (5b)$$

$$OH^-(H_2O)_3 + SO_2 \rightarrow HSO_3^- + 3H_2O \quad (6a)$$
$$\rightarrow HSO_3^-(H_2O) + 2H_2O, \quad (6b)$$

$$HCO_3^- + SO_2 \rightarrow HSO_3^- + CO_2. \quad (7)$$

The cross sections for these reactions are plotted vs the relative collision energy in Figs. 4–7. For the collision-induced dissociation processes (4a) and (5a), Figs. 8 and 9 display the energy dependence of the cross section near threshold.

In addition argon was used as the neutral target gas in

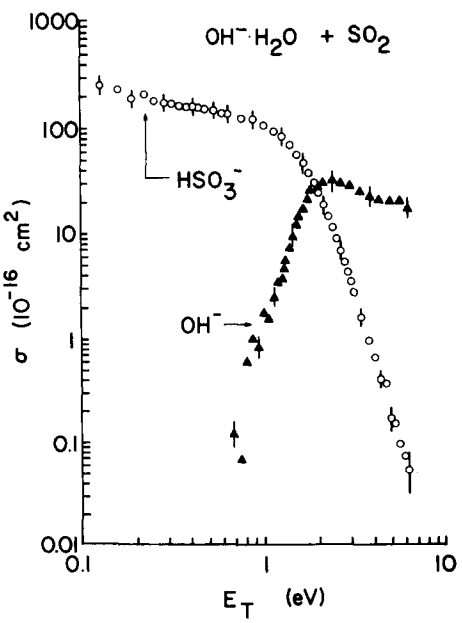


FIG. 4. Cross sections $\sigma$ for reactions (4a) ▲ and (4b) ○ as functions of the relative collision energy $E_T$.

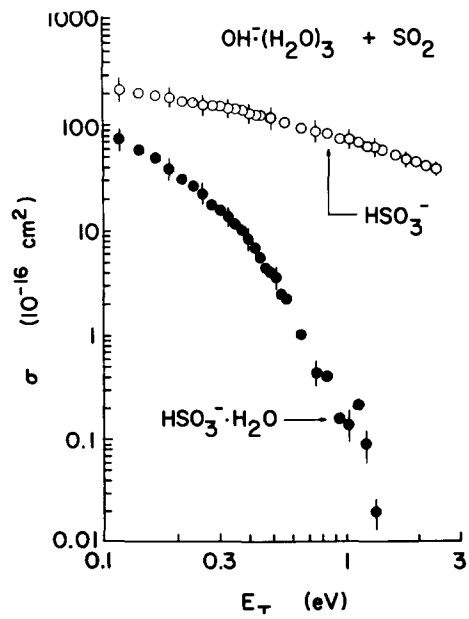


FIG. 6. Cross sections $\sigma$ for reactions (6a) ○ and (6b) ● as functions of the relative collision energy $E_T$.

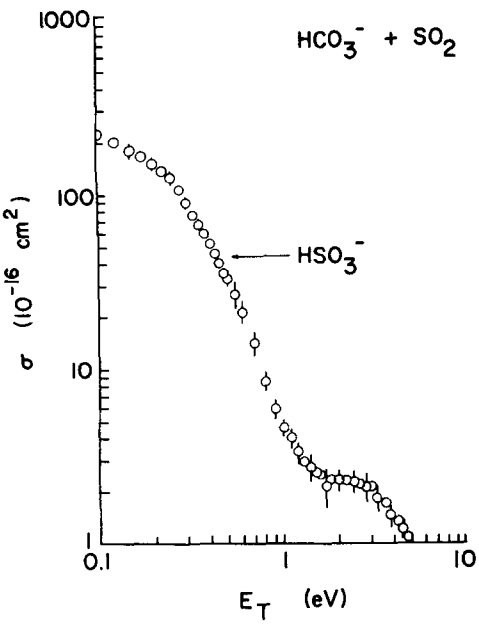


FIG. 7. Cross sections $\sigma$ for reaction (7) as a function of the relative collision energy $E_T$.

studies of the following collisional dissociation processes:

$$OH^-(H_2O) + Ar \rightarrow OH^- + H_2O + Ar, \quad (8)$$

$$HCO_3^- + Ar \rightarrow OH^- + CO_2 + Ar. \quad (9)$$

The cross sections measured for these processes are presented in Figs. 10 and 11.

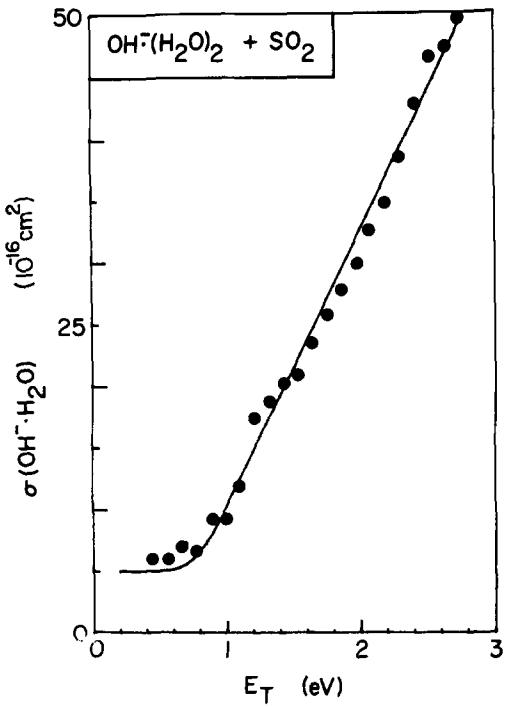


FIG. 9. Cross sections $\sigma$ for the dissociation of $OH^-(H_2O)_2$ in collisions with $SO_2$ as a function of the relative collision energy $E_T$. The solid line represents the calculated threshold behavior, as described in the text.

## IV. DISCUSSION

### A. Switching reactions

#### 1. $CO_2$

As shown in Figs. 1–3, $CO_2$ reacts rapidly with $OH^-(H_2O)_n$ ($n = 1$, 2, or 3) via solvent switching (ligand

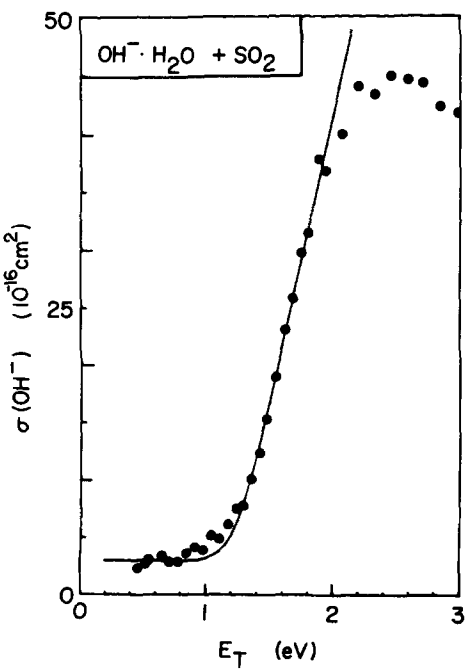


FIG. 8. Cross sections $\sigma$ for the dissociation of $OH^-(H_2O)$ in collisions with $SO_2$ as a function of the relative collision energy $E_T$. The solid line represents the calculated threshold behavior, as described in the text.

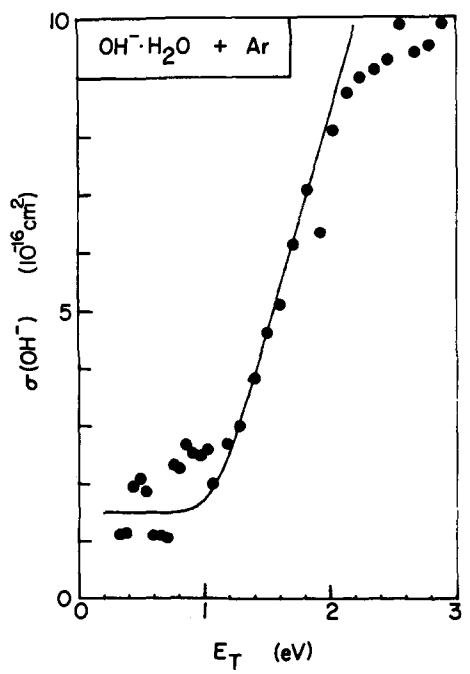


FIG. 10. Cross sections $\sigma$ for the dissociation of $OH^-(H_2O)$ in collisions with Ar as a function of the relative collision energy $E_T$. The solid line represents the calculated threshold behavior, as described in the text.

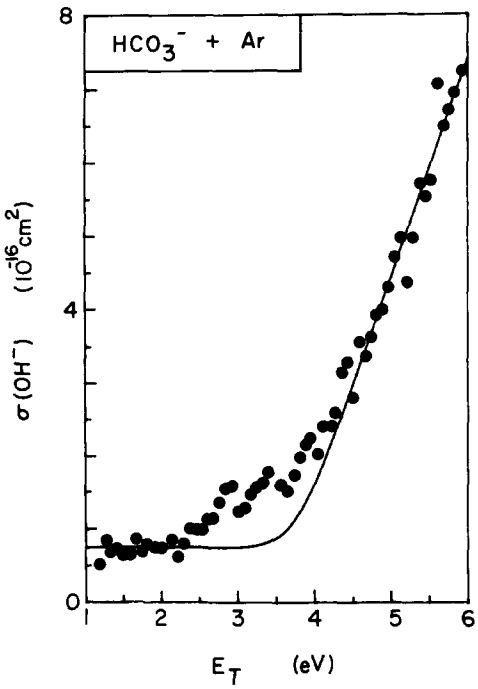


FIG. 11. Cross sections $\sigma$ for the dissociation of $HCO_3^-$ in collisions with Ar as a function of the relative collision energy $E_T$. The solid line represents the calculated threshold behavior, as described in the text.

exchange) reactions in which the $CO_2$ replaces one or more of the $H_2O$ molecules clustered to $OH^-$, leaving $HCO_3^-$ as the core ion. Strictly speaking, the product ion should be written as $OH^-(CO_2)$ if the reaction were simply ligand exchange. However, studies of the collision induced dissociation of this ion (discussed below) indicate an $OH^-$–$CO_2$ binding energy of about 3.8 eV. Since this high a binding energy indicates appreciable chemical bonding (as opposed to electrostatic attraction), we prefer to designate the product as $HCO_3^-$. In all three cases the cross sections are quite large, approaching or exceeding $100\times10^{-16}$ cm$^2$ at the very lowest collision energies. As determined from plots of log $\sigma$ vs log $E_T$, the cross sections generally decrease with increasing collision energy as $E_T^{-0.5}$ at low energies (less than about 1 eV). The cross sections decrease more rapidly at moderate energies and very rapidly (e.g. as $E_T^{-6}$) at the highest energies studied. This behavior is summarized in Table I.

With $OH^-(H_2O)$ as the reactant ion, $HCO_3^-$ is the only reaction product observed at relative collision energies less than 1 eV. At higher energies $OH^-$ produced by collisional dissociation is observed and becomes the major product at the higher energies. No attempts were made, however, to measure the cross section for its formation.

The measured cross sections for $HCO_3^-$ formation were converted to monoenergetic rate coefficients as described above, which were then plotted vs the relative collision energy (Fig. 12). Comparison with the collision rate coefficient, $8.5\times10^{-10}$ cm$^3$/molecule s, calculated from the AADO theory of Bowers and co-workers,[13] shows that the exoergic solvent switching reaction occurs on essentially every collision for collision energies less than 1 eV. As the collision energy is increased beyond this value, however, the reaction efficiency decreases; presumably this is caused by the increasing efficiency of the competing CID process, once the threshold energy for this endoergic channel has been achieved.

With $OH^-(H_2O)_2$ as the reactant ion, $HCO_3^-$ is again the major product, although nearly equivalent amounts of the hydrated product $HCO_3^-(H_2O)$ are formed at the very lowest collision energies (see Fig. 2). However, the cross section for formation of the hydrated product decreases much

TABLE I. Energy dependence of cross sections for switching reactions.

| Reaction | Slope, $\frac{d\log\sigma}{d\log E_T}$ | Applicable range of collision energies (eV) |
|---|---|---|
| $OH^-(H_2O) + CO_2 \rightarrow HCO_3^- + H_2O$ | −0.51 | 0.1–1.4 |
| | −7.1 | 4–7 |
| $OH^-(H_2O)_2 + CO_2 \rightarrow HCO_3^- + 2H_2O$ | −0.75 | 0.1–2.0 |
| $\rightarrow HCO_3^-(H_2O + H_2O$ | −3.2 | 0.2–2.5 |
| $OH^-(H_2O) + SO_2 \rightarrow HSO_3^- + H_2O$ | −0.49 | 0.1–1.0 |
| | −5.3 | 1.7–6.0 |
| $OH^-(H_2O)_2 + SO_2 \rightarrow HSO_3^- + 2H_2O$ | −0.49 | 0.1–0.5 |
| | −4.8 | 3–6 |
| $OH^-(H_2O)_3 + SO_2 \rightarrow HSO_3^- + 3H_2O$ | −0.50 | 0.1–0.5 |
| | −0.94 | 0.6–2.5 |
| $\rightarrow HSO_3^-(H_2O) + 2H_2O$ | −1.8 | 0.1–0.3 |
| | −4.2 | 0.4–1.5 |
| $HCO_3^- + SO_2 \rightarrow HSO_3^- + CO_2$ | −0.68 | 0.1–0.3 |
| | −3.8 | 0.4–1.0 |

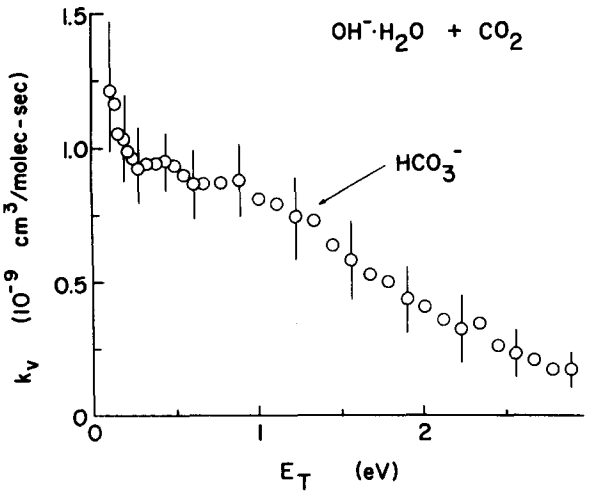


FIG. 12. Monoenergetic rate coefficients $k_v$ for reaction (1), derived from the cross sections shown in Fig. 1 by the relation $k_v = v\sigma(v)$, vs the relative collision energy $E_T$.

more rapidly with collision energy than does the cross section for $HCO_3^-$ formation. Consequently, the fractional abundance of the hydrated product decreases rapidly with increasing collision energy (see Fig. 13). At collision energies greater than 2–3 eV, CID competes effectively with solvent switching, $OH^-(H_2O)$ being the major product ion, although lesser amounts of $OH^-$ are also observed. Quantitative measurements, however, were not made for these products of collisional dissociation.

For the solvent switching reactions studied here, which can be written in general terms as

$$OH^-(H_2O)_n + XO_2 \rightarrow HXO_3^-(H_2O)_m + (n-m)H_2O, \quad (10)$$

where X = C or S, we define the fractional abundance of the solvated product at collision energy $E_T$ as

$$f_{nm}(E_T) = \frac{\sigma_m(E_T)}{\sum_{i=0}^{n} \sigma_i(E_T)} \quad (m = 1,2,\ldots,n-1), \quad (11)$$

where $\sigma_i(E_T)$ is the cross section for formation of $HXO_3^-(H_2O)_i$ at energy $E_T$. It was found (see e.g., Fig. 13), that the energy dependence of the fractional abundance could be approximated by the empirical relation.

$$f_{nm}(E_T) = f^\circ_{nm} \exp(-E_T/E_{nm}), \quad (11a)$$

where $f^\circ_{nm}$ is the abundance extrapolated to zero collision energy, and $E_{nm}$ is the increase in relative translational energy which causes the fractional abundance to decrease by a factor of $1/e$. For reaction (2), the values of these parameters, derived from Fig. 13, are $f^\circ_{21} = 0.44$ and $E_{21} = 0.22$ eV. Values of these parameters for the other solvent switching reactions studied are listed in Table II.

TABLE II. Fractional abundance, $f_{nm}(E_T) = f^\circ_{nm}\exp(-E_T/E_{nm})$ for solvent switching reactions of the general type.

| | $OH^-(H_2O)_n + XO_2 \rightarrow HXO_3^-(H_2O)_m + (n-m)H_2O$ | | | |
|---|---|---|---|---|
| X | $n$ | $m$ | $f^\circ_{nm}$ | $E_{nm}$(eV) |
| C | 2 | 1 | 0.44 | 0.22 |
| C | 3 | 2 | 0.075 | 0.19 |
| C | 3 | 1 | 0.74 | 1.06 |
| S | 3 | 1 | 0.51 | 0.18 |

Derived monoenergetic rate coefficients for reaction (2) are plotted vs $E_T$ in Fig. 14. Comparison with the calculated collision rate coefficient[13] of $7.7\times10^{-10}$ cm$^3$/molecule s again shows that the exoergic solvent switching process occurs with essentially unit efficiency at low collision energies, although this efficiency starts to decrease once the threshold for CID is exceeded.

Similar results are also found for the reaction of $OH^-(H_2O)_3$ with $CO_2$ (see Fig. 3). At the lowest collision

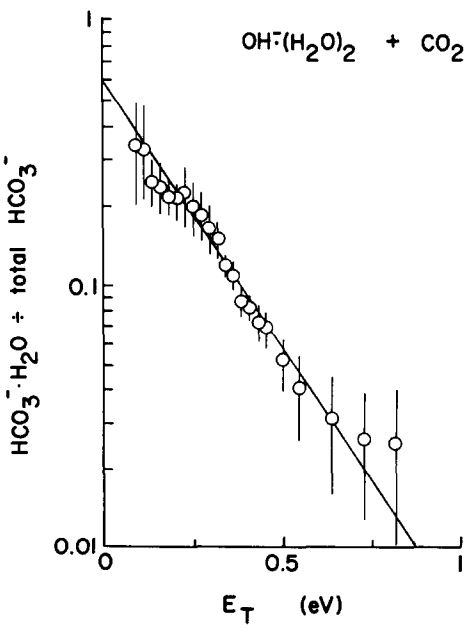


FIG. 13. Fractional abundance $f_{21}(E_T)$ of the solvated product $HCO_3^-(H_2O)$ formed in the solvent switching reactions between $OH^-(H_2O)_2$ and $CO_2$ vs the relative collision energy $E_T$. The solid line represents the best fit to the points of the empirical relation given by Eq. (11).

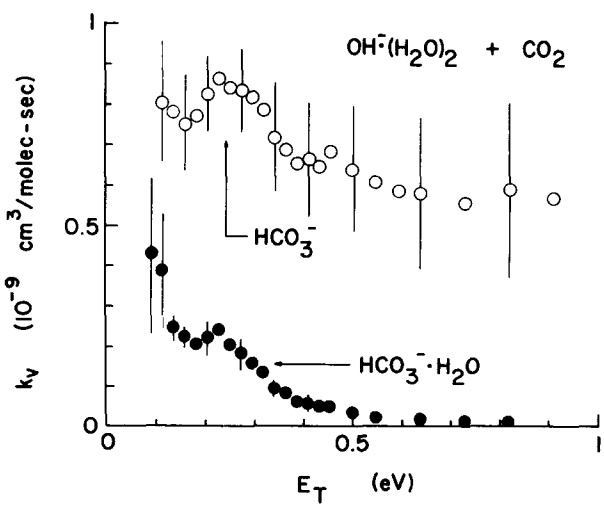


FIG. 14. Monoenergetic rate coefficients $k_v$ for reactions (2a) ○ and (2b) ●, derived from the cross sections shown in Fig. 2, vs the relative collision energy $E_T$.

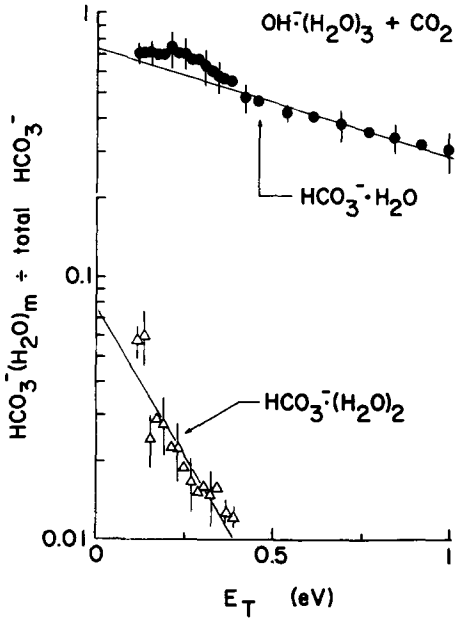


FIG. 15. Fractional abundances $f_{3m}(E_T)$ of the solvated products $HCO_3^-(H_2O)_m$ ($m = 1$ or 2) formed in the solvent switching reactions between $OH^-(H_2O)_3$ and $CO_2$. The straight lines represent the best fit of Eq. (11) to the experimental data.

energies, the dominant product ion is $HCO_3^-(H_2O)$, formed by the exchange of $CO_2$ for two $H_2O$ molecules; appreciable amounts of $HCO_3^-$ but only minor amounts of $HCO_3^-(H_2O)_2$ are observed. As the collision energy is increased, however, the cross sections for the hydrated products fall rapidly, again leaving the unsolvated ion $HCO_3^-$ as the principal product. As can be seen from Fig. 15, the fractional abundances of the solvated products $HCO_3^-(H_2O)_m$ (where $m = 1$ or 2) once again show an exponential dependence (Eq. (11)] upon the collision energy. The derived values for the parameters $f^*_{nm}$ and $E_{nm}$ are listed in Table II. Monoenergetic rate coefficients for reactions (3a) and (3b) are plotted vs $E_T$ in Fig. 16. Comparison with the AADO

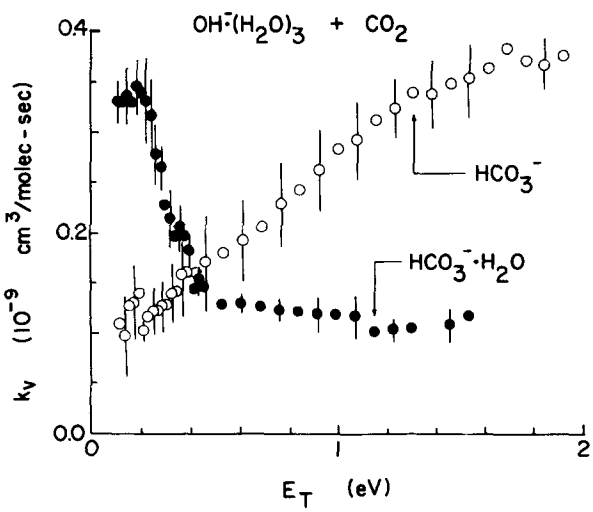


FIG. 16. Monoenergetic rate coefficients $k_v$ for reactions (3a) ○ and (3b) ●, derived from the cross sections shown in Fig. 3, vs the relative collision energy $E_T$.

collision rate coefficient, $7.2 \times 10^{-10}$ cm$^3$/molecule s, shows that $HCO_3^-(H_2O)$ production occurs with a reaction efficiency of about 1/2 at the very lowest energies, while $HCO_3^-$ production is considerably less efficient. As the collision energy is increased, the efficiency of $HCO_3^-$ production increases, apparently at the expense of $HCO_3^-(H_2O)$ production, which decreases markedly with increasing collision energy. At no point, however, does the sum of the rate coefficients for these solvent switching reactions equal the collision rate coefficient, suggesting that the addition of the third water molecule to the reactant $OH^-$ ion precludes solvent transfer in a significant fraction (perhaps 1/3) of the collisions. Although this is to be expected at the higher collision energies, where CID competes effectively with solvent switching, it stands in contrast to the low-energy results for reactions (1) and (2), where solvent switching occurs on essentially every collision.

This propensity for a single $CO_2$ molecule to replace two or even three water molecules has been observed previously in the thermal energy experiment by Fehsenfeld and Ferguson,[3] although they were unable to determine the exact degree of $H_2O$ loss because of subsequent reactions of the product ions in their flowing afterglow system. They suggested, however, and the present results would seem to confirm, that these solvent switching reactions are sufficiently exothermic that the replacement of a single $H_2O$ molecule by $CO_2$ leaves the ionic products with enough internal energy to "boil off" one or more additional water molecules.

Using literature values[11,12] for the enthalpy changes associated with the clustering of water molecules to $OH^-$ and $HCO_3^-$, and assuming the value of 3.8 eV determined in this study for $D(OH^- - CO_2)$, we have calculated enthalpy changes for the switching reactions of $OH^-(H_2O)_n$ with $CO_2$. We find, for example, that the reaction

$$OH^-(H_2O)_2 + CO_2 \rightarrow HCO_3^-(H_2O) + H_2O \qquad (2b)$$

is exothermic by 2.62 eV, and the reaction

$$OH^-(H_2O)_3 + CO_2 \rightarrow HCO_3^-(H_2O)_2 + H_2O \qquad (3c)$$

is exothermic by 2.61 eV. Since 0.65 eV is required to remove a molecule of water from $HCO_3^-(H_2O)_2$, and 0.68 eV for the removal of water from $HCO_3^-(H_2O)$, only a fraction of the reaction exothermicity need be partitioned into internal energy of the nascent ionic products of reactions (2b) and (3c) to cause their subsequent decomposition before reaching the detector. Since the internal energy of the reaction products is likely to increase with increasing collision energy, one would expect the observed enhancement of $HCO_3^-$ relative to $HCO_3^-(H_2O)$ and $HCO_3^-(H_2O)_2$ at higher collision energies.

As described above, the cross sections $\sigma$ for these reactions were converted to monoenergetic rate coefficients by application of the relation $k(v_r) = v_r\sigma(v_r)$, and then extrapolated to thermal energies to obtain pseudo thermal energy rate coefficients. The results are listed in Table III, along with the experimental values obtained previously by Fehsenfeld and Ferguson[3] and with values calculated using the AADO theory of Bowers and co-workers.[13]

The present results indicate that $OH^-(H_2O)_2$ reacts with $CO_2$ at about the same rate as does $OH^-(H_2O)$. How-

TABLE III. Rate coefficients for switching reactions.

| Reaction | Rate coefficient This work[a] | $k \times 10^{10}$ cm³/molecule s Previous work[b] | Calculated[c] |
|---|---|---|---|
| $OH^-(H_2O) + CO_2 \rightarrow HCO_3^- + H_2O$ | $10 \pm 3$ | ... | 8.5 |
| $OH^-(H_2O)_2 + CO_2 \rightarrow HCO_3^- + 2H_2O$ | $8 \pm 2$ | | |
| | | 6 | 7.7 |
| $\rightarrow HCO_3^-(H_2O) + H_2O$ | $3.5 \pm 1$ | | |
| $OH^-(H_2O)_3 + CO_2 \rightarrow HCO_3^- + 3H_2O$ | $1.1 \pm 0.3$ | | |
| $\rightarrow HCO_3^-(H_2O) + 2H_2O$ | $3.4 \pm 1.0$ | 6 | 7.2 |
| $\rightarrow HCO_3^-(H_2O)_2 + H_2O$ | $0.25 \pm 0.10$ | | |
| $OH^-(H_2O) + SO_2 \rightarrow HSO_3^- + H_2O$ | $23 \pm 6$ | ... | |
| $OH^-(H_2O)_2 + SO_2 \rightarrow HSO_3^- + 2H_2O$ | $22 \pm 5$ | | |
| | | 20 | 16 |
| $\rightarrow HSO_3^-(H_2O) + H_2O$ | ... | | |
| $OH^-(H_2O)_3 + SO_2 \rightarrow HSO_3^- + 3H_2O$ | $14 \pm 3$ | | |
| $\rightarrow HSO_3^-(H_2O) + 2H_2O$ | $8 \pm 2$ | 20 | 15.0 |
| $\rightarrow HSO_3^-(H_2O)_2 + H_2O$ | ... | | |
| $HCO_3^- + SO_2 \rightarrow HSO_3^- + CO_2$ | $17.5 \pm 2.0$ | ... | 15.6 |

[a] Derived by converting the measured cross sections to monoenergetic rate constants, $k(v_r) = v_r\sigma(v_r)$, and then extrapolating to thermal energies.
[b] Reference 3.
[c] Calculated from AADO theory [Eq. (27), Ref. 13], using the following data: dipole moments 1.63 and 0.0 D for $SO_2$ and $CO_2$, respectively (Ref. 16); molecular polarizabilities: $3.72 \times 10^{-24}$ and $2.65 \times 10^{-24}$ cm³ for $SO_2$ and $CO_2$, respectively (Ref. 17). Moments of inertia were calculated from structural data in Ref. 18.

ever, $OH^-(H_2O)_3$ reacts noticeably more slowly with $CO_2$ than does $OH^-(H_2O)$. Fehsenfeld and Ferguson,[3] on the other hand, reported no appreciable difference in the reactivity of $OH^-(H_2O)_n$ as $n$ was changed from 2 to 4. Because AADO theory predicts a rate coefficient which will vary inversely with the square root of the reduced mass of the reactants, one might anticipate a slight decrease in rate with increasing solvation; the decrease we observe, however, is clearly greater than that expected solely on the basis of increases in the reduced masses of the reactants.

### 2. $SO_2$

As shown in Figs. 4–6, $SO_2$ also reacts rapidly with $OH^-(H_2O)_n$ ($n = 1,2$, or 3) via solvent switching reactions in which the $SO_2$ replaces one or more of the $H_2O$ molecules, leaving $HSO_3^-$ as the core ion. These reactions appear to be even more rapid than the analogous reactions of $CO_2$, with the cross sections exceeding $100 \times 10^{-16}$ cm² at the lowest collision energies. Again, the cross sections decrease with increasing collision energy, varying as $E_T^{-0.5}$ at low energies

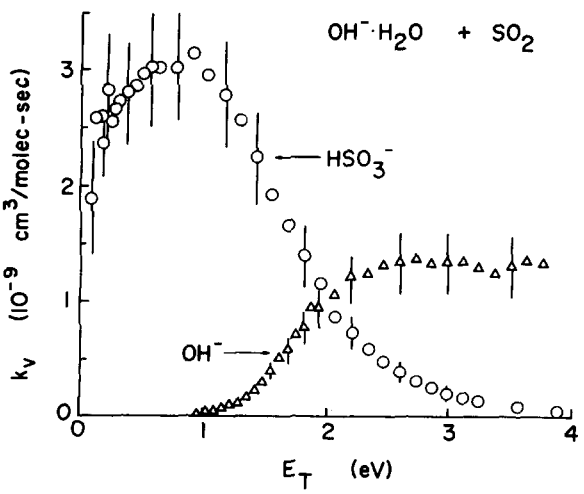


FIG. 17. Monoenergetic rate coefficients $k_v$ for reactions (4a) △ and (4b) ○, derived from the cross sections shown in Fig. 4, vs the relative collision energy $E_T$.

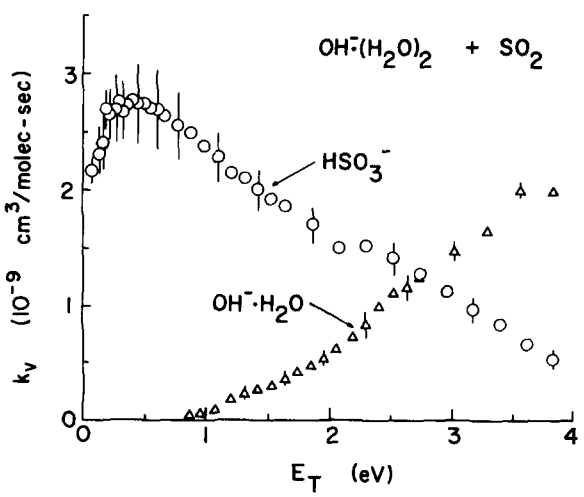


FIG. 18. Monoenergetic rate coefficients $k_v$ for reactions (5a) △ and (5b) ○, derived from the cross sections shown in Fig. 5, vs the relative collision energy $E_T$.

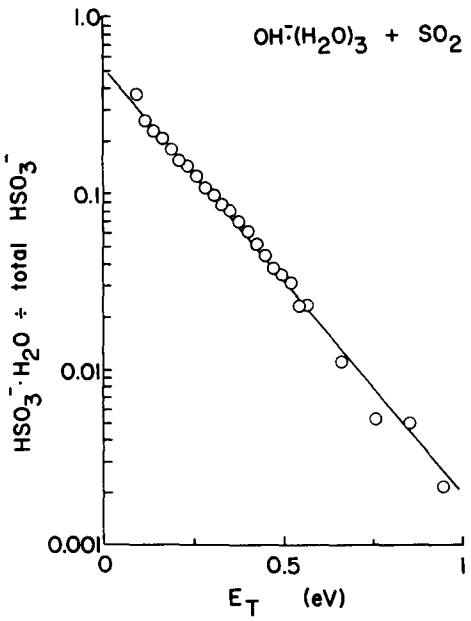


FIG. 19. Fractional abundance $f_{31}(E_T)$ of the solvated product $HSO_3^-(H_2O)$ formed in the solvent switching reactions between $OH^-(H_2O)_3$ and $SO_2$ vs the relative collision energy $E_T$. The straight line represents the best fit of Eq. (11) to the experimental data.

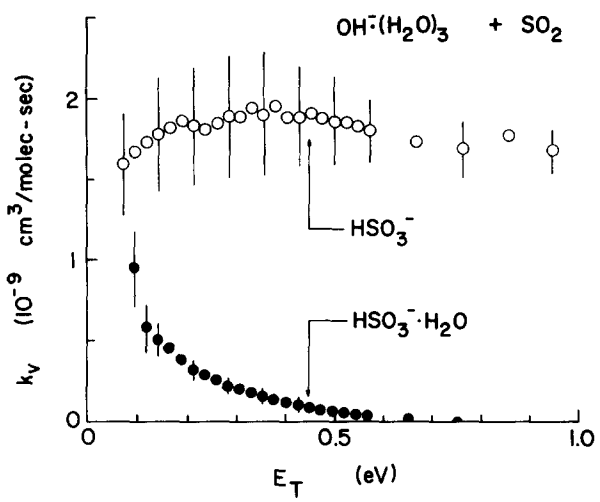


FIG. 20. Monoenergetic rate coefficients $k_v$ for reactions (6a) ○ and (6b) ●, derived from the cross sections shown in Fig. 6, vs the relative collision energy $E_T$.

and falling much more rapidly at higher energies (see Table I). At collision energies greater than 1.5–2.0 eV, cross sections for the collisional dissociation of the solvated reactant ion become greater than those for solvent switching.

The competition between solvent switching and CID, and the effective quenching of the former channel by the latter at higher collision energies is clearly seen in Figs. 17 and 18, which show $k(v_r)$ vs $E_T$ for reactions (4) and (5), respectively. At collision energies below the threshold for CID (i.e., $E_T < 1$ eV), the monoenergetic rate coefficients for $HSO_3^-$ formation are essentially constant and of such a magnitude that solvent switching appears to occur on every collision. At higher energies, however, there is a precipitous decline in the reaction efficiency for $HSO_3^-$ production. This decline is accompanied by a rapid increase in the efficiency of the CID process, so that a majority of the collisions lead to collisional dissociation of the reactant ion rather than solvent switching at collision energies greater than about 2.5 eV.

The extent of $H_2O$ loss from the ionic product of these switching reactions with $SO_2$ is even more extensive than in analogous reactions of $CO_2$. $HSO_3^-$ is the sole observed product in the reactions of $OH^-(H_2O)$ and $OH^-(H_2O)_2$ with $SO_2$; only minor amounts of $HSO_3^-(H_2O)$ and no $HSO_3^-(H_2O)_2$ were observed with $OH^-(H_2O)_3$ as the reactant ion. As shown in Fig. 19, the dramatic decrease in the fractional abundance of $HSO_3^-(H_2O)$ with increasing collision energy for the latter system is well described by the empirical relation expressed by Eq. (11). The derived values of the parameters are $f'_{31} = 0.51$ and $E_{31} = 0.18$ eV. The suggestion that solvent boil-off contributes to the decreased production of the solvated product at higher collision energies is supported by consideration of the energy dependence of the monoenergetic rate coefficients for reaction (6). As shown in Fig. 20, the rapid decrease in reaction efficiency for $HSO_3^-(H_2O)$ production with increasing energy is mirrored by an increase in the efficiency of $HSO_3^-$ production. These observations suggest that the reactions of $SO_2$ with $OH^-(H_2O)_n$ are even more exothermic than those of $CO_2$. This suggestion is confirmed by the observation that the switching reaction

$$HCO_3^- + SO_3 \rightarrow HSO_3^- + CO_2 \qquad (8)$$

proceeds very rapidly at even the lowest energies studied and has a cross section that decreases monotonically with increasing collision energy (see Fig.7). Since such behavior is characteristic of exothermic ion-molecule reactions, we conclude that $D(OH^- - SO_2) > D(OH^- - CO_2) = 3.8$ eV.

As shown in Table III, the pseudo thermal energy rate coefficients derived from the cross sections for these reactions measured in the present study are comparable to those reported previously by Fehsenfeld and Ferguson[3] and those predicted by AADO theory.[13] The present results are in agreement with the previous finding[3] that increased solvation of the $OH^-$ reactant has no appreciable effect on the rates of these reactions with $SO_2$, and that $SO_2$ reacts 2–3 times more rapidly with $OH^-(H_2O)_n$ than does $CO_2$. According to AADO theory, this latter observation can be attributed to the fact that $SO_2$ possesses a permanent dipole moment while $CO_2$ does not.

### B. Collision-induced dissociation

Cross sections were measured for the collisional dissociation processes listed in Sec. III. These processes, which result in the loss of one or more $H_2O$ molecules from the $OH^-(H_2O)_n$ reactant, are the dominant processes occurring at relative collision energies greater than 1.5–2.0 eV. Moreover, interpretation of the energy dependence of the cross sections for these endothermic reactions in the vicinity of threshold can provide information on both the binding energies of the solvent molecules to the core ion and the extent of internal excitation of the $OH^-(H_2O)_n$ reactant ions.

In order to interpret these experiments accurately, the

TABLE IV. Threshold behavior, $\sigma(E_T) = Q(E_T - E_0)$ for collision induced dissociation.

| Reaction | Parameters $Q$(Å²/eV) | $E_0$(eV) | Expected threshold (eV) |
|---|---|---|---|
| $OH^-(H_2O) + SO_2 \rightarrow OH^- + H_2O + SO_2$ | 49.5 | $1.25 \pm 0.10$ | 1.08[a] |
| $OH^-(H_2O) + Ar \rightarrow OH^- + H_2O + Ar$ | 7.5 | $1.12 \pm 0.10$ | 1.08[a] |
| $OH^-(H_2O)_2 + SO_2 \rightarrow OH^-(H_2O) + H_2O + SO_2$ | 22.3 | $0.80 \pm 0.10$ | 0.79[a] |
| $HCO_3^- + Ar \rightarrow OH^- + CO_2 + Ar$ | 3.0 | $3.8 \pm 0.25$ | 2.43[b] |

[a] Reference 11.
[b] Reference 15.

effect of the thermal motion of the target gas molecules must be taken into account. This can be done by assuming a functional form for the true microscopic reaction cross section, convoluting this assumed cross section with the experimental conditions, and then comparing the results with the phenomenological cross section.

We have assumed that the true cross sections $\sigma(E_T)$ for these processes increase linearly with relative translational energy $E_T$ above the threshold value $E_0$ according to the equation

$$\sigma(E_T) = \begin{cases} 0 & \text{if } E_T < E_0 \\ Q(E_T - E_0) & \text{if } E_T \geq E_0 \end{cases} \quad (12)$$

Assuming that a monoenergetic ion beam interacts with target gas molecules having an isotropic Maxwellian velocity distribution, we have convoluted the assumed cross section with the distribution in relative velocities according to the procedure described by Chantry [Eq. (30), Ref. 14]. The results were then compared with the phenomenological cross sections, and the parameters $Q$ and $E_0$ were varied until satisfactory agreement was achieved. The results are shown in Figs. 8–11, and are summarized in Table IV.

The derived thresholds for the dissociation of $OH^-(H_2O)$ and $OH^-(H_2O)_2$ are in good agreement with the values expected from the equilibrium studies of Kebarle and co-workers,[11] while that observed for the dissociation of $HCO_3^-$ is considerably higher than the theoretical value of 2.4 eV from the *ab initio* calculations of Jönsson *et al.*[15]

As the calculations (solid lines) show, much of the observed tailing of the measured cross sections at collision energies below threshold can be attributed to the effect of the thermal motion of the target gas molecules. The fact that the cross sections are nonzero at relative energies considerably below the expected thresholds is thought to be due principally to energetic collisions occurring outside the collision chamber, in a region where gas is streaming out the exit orifice of the collision chamber. There may also be a contribution of these cross sections from excited reactant ions. In the cases of $OH^-(H_2O)$ and $OH^-(H_2O)_2$, however, the generally good agreement between observed cross sections and those calculated on the assumption of a linear increase above threshold suggests that the great majority of these reactant ions possess little if any internal excitation by the time they are extracted from the ion source. On the other hand, the observed cross sections for the collisional dissociation of $HCO_3^-$ (Fig. 11) show more extensive tailing below threshold than can be explained solely by the thermal motion of the target gas. This observation suggests that a significant fraction of these reactant ions might possess considerable internal energy when they leave the ion source. Since $HCO_3^-$ is produced in the ion source by the very exothermic reactions of $OH^-(H_2O)_n$ with $CO_2$, we would not expect the resulting $HCO_3^-$ to be completely thermalized by the time it is extracted under the conditions at which our source was operated.

### C. Charge transfer reactions

#### 1. $CO_2$

No charge transfer reaction was observed between $OH^-$ and $CO_2$. This is to be expected; although $CO_2^-$ has been detected in high energy processes in which the linear neutral $CO_2$ can be bent to form the ion,[19] the $CO_2^-$ ion is short lived[20] and autodetaches to form the linear ground state of $CO_2$.

#### 2. $SO_2$

The endoergic charge transfer process

$$OH^- + SO_2 \rightarrow SO_2^- + OH \quad (13)$$

was observed at relative collision energies greater than 1 eV. Although the quality of the data was inadequate for an accurate determination of the threshold energy, one can calculate a threshold energy of 0.728 eV using the reported values of 1.825[21] and 1.097 eV[22] for the electron affinities of OH and $SO_2$, respectively. Above onset, the measured cross section for reaction (13) rose to a maximum value of about 7 Å² at $E_T \sim 3.5$ eV, and then gradually decreased to $\sim 3$ Å² at $E_T = 15$ eV.

With $OH^-(H_2O)$ as the reactant ion, the charge transfer process

$$OH^-(H_2O) + SO_2 \rightarrow SO_2^- + OH + H_2O \quad (14)$$

was observed as a minor reaction channel with cross sections gradually increasing to about 2 Å² at collision energies 5 eV above threshold (calculated to be 1.81 eV). Charge transfer with solvent transfer,

$$OH^-(H_2O) + SO_2 \rightarrow SO_2^-(H_2O) + OH \quad (15)$$

was not detected in the present study.

These findings differ appreciably from those reported[6] previously for the reactions of $NO_2$ with $OH^-(H_2O)$, the salient features of which were: (1) charge transfer to yield $NO_2^-$ was the major reaction channel ($\sigma > 20$ Å²) at collision energies greater than 1 eV; (2) charge transfer with solvent transfer to give $NO_2^-(H_2O)$ was an important channel

between 0.3 and 2 eV; (3) CID did not compete effectively with charge transfer and hence was not an important reaction channel even at high collision energies ($\sim 5$ eV).

## V. SUMMARY

Cross sections for the reactions of $OH^-(H_2O)_n$ $(0 \leqslant n \leqslant 3)$ with $CO_2$ and $SO_2$ have been measured over the range of reactant translational energy 0.15–25.0 eV (LAB). At low energies ($E_T < 1$ eV), the dominant processes are solvent switching reactions in which the neutral reactant replaces one or more of the $H_2O$ solvent molecules, leaving $HCO_3^-$ or $HSO_3^-$ as the core ion. These reactions are very rapid, occurring essentially on every collision, and increasing solvation of the reactant ion has little or no effect on the rate. The only exception would appear to be reaction (3), where the addition of a third $H_2O$ molecule to the $OH^-$ reactant ion noticeably decreases the rate with which it undergoes solvent switching with $CO_2$. The unsolvated ions $HCO_3^-$ and $HSO_3^-$ are found to be the principal products in all cases except reaction (3), where the fractional abundance of $HCO_3^-(H_2O)$ exceeds that of $HCO_3^-$ at the very lowest collision energies. The failure of these systems to form the energetically more favorable solvated ionic products is attributed to the rather high exothermicity of these reactions, which causes extensive boil off of the $H_2O$ solvent molecules.

At higher collision energies (above 1–2 eV), collision-induced dissociation of the reactant ion becomes the major reaction channel. Analysis of the excitation functions near threshold for these endothermic processes yields values for the bond dissociation energies of these cluster ions which are in generally good agreement with the values obtained by other methods.

## ACKNOWLEDGMENTS

We wish to acknowledge useful discussions with Professor M. J. Henchman on ion solvation. We are grateful to F. Dale for his efforts in modifying and maintaining the double mass spectrometer. We thank J. A. Welsh for development of a computer program used in performing the measurements. This work was supported in part by the Defense Nuclear Agency.

[1] F. C. Fehsenfeld and D. L. Albritton, *Atmospheric Water Vapor*, edited by A. Deepak, T. D. Wilkerson, and L. H. Ruhnke (Academic, New York, 1980), pp. 587–597.
[2] E. E. Ferguson and F. Arnold, Acc. Chem. Res. **11**, 327 (1981).
[3] F. C. Fehsenfeld and E. E. Ferguson, J. Chem. Phys. **61**, 3181 (1974).
[4] R. M. Beall, PB Report No. 241 493, 1975, U.S. NTIS.
[5] See, for example, D. R. Strome, R. L. Clancy, and N. C. Garzales, J. Appl. Physiol. **43**, 925 (1977).
[6] J. F. Paulson and F. Dale, J. Chem. Phys. **77**, 4006 (1982).
[7] J. F. Paulson, J. Chem. Phys. **52**, 959 (1970).
[8] J. F. Paulson and P. J. Gale, Adv. Mass Spectrom. **A7**, 263 (1978).
[9] The relative collision energy $E_T$ was calculated by assuming a stationary target. That is, $E_T = mE_L/(M+m)$, where $m$ and $M$ are the masses of the neutral and the ionic reactants, respectively, and $E_L$ is the most probable laboratory translational energy of the ionic reactant.
[10] See, for example, *Interaction Between Ions and Molecules*, edited by P. Ausloos (Plenum, New York, 1975), pp. 595–618.
[11] J. D. Payzant, R. Yamdagni, and P. Kebarle, Can. J. Chem. **49**, 3308 (1971).
[12] R. G. Keesee, N. Lee, and A. W. Castleman, Jr., J. Am. Chem. Soc. **101**, 2599 (1979).
[13] T. Su, E. C. F. Su, and M. T. Bowers, J. Chem. Phys. **69**, 2245 (1978).
[14] P. J. Chantry, J. Chem. Phys. **55**, 2746 (1971).
[15] B. Jönsson, G. Karlström, and H. Wennerström, J. Am. Chem. Soc. **100**, 1658 (1978).
[16] R. D. Nelson, Jr., D. R. Lide, Jr., and A. A. Maryott, Natl. Stand. Ref. Data Ser. Natl. Bur. Stand. **10** (1967).
[17] *Landolt–Börnstein, Zahlenwerte und Funktionen* (Springer, Berlin, 1951), Vol. 1, Part 3, p. 510.
[18] G. Herzberg, *Molecular Spectra and Molecular Structure. II. Infrared and Raman Spectra of Polyatomic Molecules* (Van Nostrand, Princeton, 1966).
[19] J. F. Paulson, J. Chem. Phys. **52**, 963 (1970).
[20] R. N. Compton, P. W. Reinhardt, and C. D. Cooper, J. Chem. Phys. **60**, 2953 (1974).
[21] H. Hotop, T. A. Patterson, and W. C. Lineberger, J. Chem. Phys. **60**, 1806 (1974).
[22] R. J. Celotta, R. A. Bennett, and J. L. Hall, J. Chem. Phys. **60**, 1740 (1974).